

Spontaneous Dissociation of Streptavidin from Biotinylated Double Stranded DNA

Michelle A. Kennedy

Committee Members

Dr. Robert Kuchta: Department of Chemistry and Biochemistry

Dr. Joseph Falke: Department of Chemistry and Biochemistry

Dr. Robert Garcea: Department of Molecular, Cellular, and Developmental Biology

Undergraduate Thesis

Spring 2017

Thesis Advisor: Dr. Robert Kuchta

University of Colorado at Boulder

Department of Chemistry and Biochemistry

Acknowledgements

First and foremost, I owe infinite thanks and gratitude to my mentor, Rob Kuchta. From your endless patience in answering the most trivial of questions, to giving me the opportunity to be an independent researcher, I cannot express how grateful I am to have such a wonderful friend, mentor, and teacher in my life. For similar reasons, I need to thank the members of the Kuchta Lab, especially Sarah Dickerson, for their endless support of my projects and for being great company at the bench. Thank you to the Luger Lab, particularly Johannes Rudolph, for letting us use your fluorescence polarization equipment. Additionally, thank you to Jake Polaski and Neil Lloyd of the Batey and Wuttke Labs, respectively, for their help with modeling the streptavidin-biotinylated DNA interaction. Finally, thank you to my honors committee—Joe Falke and Bob Garcea—for taking the time to evaluate my performance as an undergraduate researcher.

To my friends and family, your support of my pursuit of a scientific career has meant more than you will ever know. Thank you for listening to my ramblings, even when you only understand ten percent of what I am saying, and for continuing to come to my presentations after all these years. I am so excited to be heading to grad school to pursue my Ph.D., and I cannot wait to see what the future has in store.

Table of Contents

I.	Abstract	3
II.	Introduction	4
	<i>STREPTAVIDIN AND AVIDIN: A BRIEF HISTORY</i>	4
	<i>STRUCTURAL ORIGINS OF HIGH AFFINITY BINDING</i>	5
	<i>BIOTIN-MODIFICATION OF BIOLOGICAL SUBSTRATES</i>	6
	<i>EXPLOITATION OF THE STREPTAVIDIN-BIOTIN COMPLEX</i>	8
	<i>IN THE LABORATORY</i>	
	<i>DISSOCIATION OF STREPTAVIDIN FROM BIOTINYLATED DNA</i>	8
III.	Materials and Methods	9
	<i>DNA OLIGOS</i>	9
	<i>DNA PURIFICATION</i>	10
	<i>5' RADIOLABELING OF BIOTINYLATED DNA AND</i>	10
	<i>DUPLEX PREPARATION</i>	
	<i>ELECTROPHORETIC MOBILITY SHIFT ASSAYS (EMSA)</i>	10
	<i>FLUORESCENCE POLARIZATION ASSAYS</i>	11
IV.	Results	12
V.	Discussion and Conclusions	18
VI.	References	24

Abstract

The binding of streptavidin to biotin is one of the strongest non-covalent interactions observed in nature. However, we have observed that streptavidin rapidly dissociates from biotinylated double stranded DNA in the presence of free biotin. In contrast, streptavidin does not rapidly dissociate from single stranded biotinylated DNA under identical conditions. Due to the ubiquitous exploitation of the streptavidin-biotin system in the laboratory, we investigated this phenomenon in greater detail. To study the dissociation of streptavidin from biotinylated DNA, we used fluorescence polarization and electrophoretic mobility shift assays. We found that the binding of streptavidin to double stranded DNA can be stabilized by one or more mismatches across from the biotinylated site. Moreover, molecular modeling of the interaction suggests that steric and electrostatic effects may play a role in catalyzing streptavidin dissociation. We propose that the weaker interaction between streptavidin and double stranded DNA is stabilized by mismatches because they make the DNA more locally fluid, and thus allow the DNA to adopt a more sterically and electrostatically favorable orientation in relation to streptavidin. More investigation is necessary to validate these speculations, but, regardless, these findings are valuable to the scientific community.

Introduction

Streptavidin and avidin: A brief history

Streptavidin (SA) is a homotetrameric protein isolated from the bacterium *Streptomyces avidinii* that is best known for its ability to form a strong non-covalent interaction with the growth factor biotin (also known as vitamin H/B7 or coenzyme R) [1]. In fact, with a K_D on the order of 10^{-14} M, the interaction between SA and biotin is one of the strongest non-covalent interactions that exists in nature [2]. For this reason, this complex is frequently exploited in the laboratory setting, and numerous genetically engineered SA-like proteins have been developed that exhibit enhanced binding properties, such as increased biotin affinity or functional monomeric or monovalent SA mutants [3, 4, 5, 6].

SA is structurally similar to another biotin-binding protein, avidin, which preceded SA in discovery. Avidin is isolated from avian and amphibian egg whites and is thought confer antibiotic properties [1]. The biological function of SA is unknown—however, it is believed to impart similar antibiotic qualities. Although avidin and SA share some amino acid homology (approximately 30 percent), the secondary and tertiary structures of the two proteins are remarkably similar [8]. The primary difference between the two proteins is in their post-translational modifications. In particular, SA lacks glycosylation, which results in less non-specific binding and makes SA more useful in laboratory applications than avidin [1].

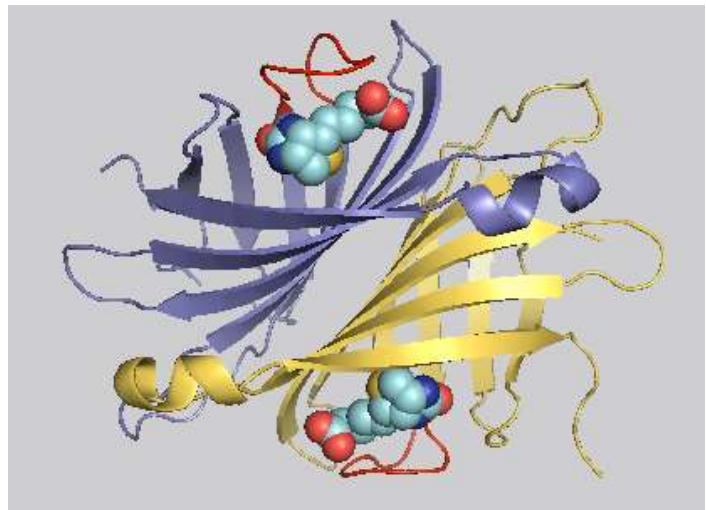


Figure 1: Structural representation of one SA dimer bound to biotin. Biotin is shown in space-filling mode and the flexible binding loops are indicated in red (modified from Le Trong et al. 2011 and edited in Pymol) [7].

Structural origins of high affinity binding

There are many structural aspects of SA that allow it to tightly bind biotin. However, the anomalous strength of this bond is still being investigated [9, 10]. Three types of interactions have been identified that seem to account for the high affinity binding of biotin to SA (*Fig. 2*). First, there is extensive hydrogen bonding between biotin and polar residues within the binding pocket of SA. SA residues N23, S27, Y43, S88, T90 and D128 have been shown to hydrogen bond with biotin via its ureido and terminal carbonyl groups [11]. Second, there are multiple tryptophan residues (W79, 92, 108 and 120) that are believed to contribute to binding via strong hydrophobic interactions [12]. W120 is donated from an adjacent SA subunit and thus is believed to contribute to cooperativity and SA subunit communication upon biotin binding [13]. It should be noted, however, that there does not seem to be a consensus about whether SA subunits bind biotin in a cooperative manner [9, 14, 15].

Finally, a conformational change of the flexible binding loop between β strands 3 and 4 is thought to close over bound biotin and further stabilize its binding to SA. However, instead of interacting directly with the biotin, it is believed that intramolecular interactions within the protein are primarily responsible for the increase in binding strength [16]. Residues S45, V47, G48, N49 and A50 seem to be particularly important and make hydrogen bonding contacts with other SA residues [7, 16, 17].

Interestingly, the conformational change of the binding loop is practically the only large-scale conformational change that is observed upon biotin binding. In general, there are only local conformational changes upon binding, but a general overall contraction of the protein occurs [7].

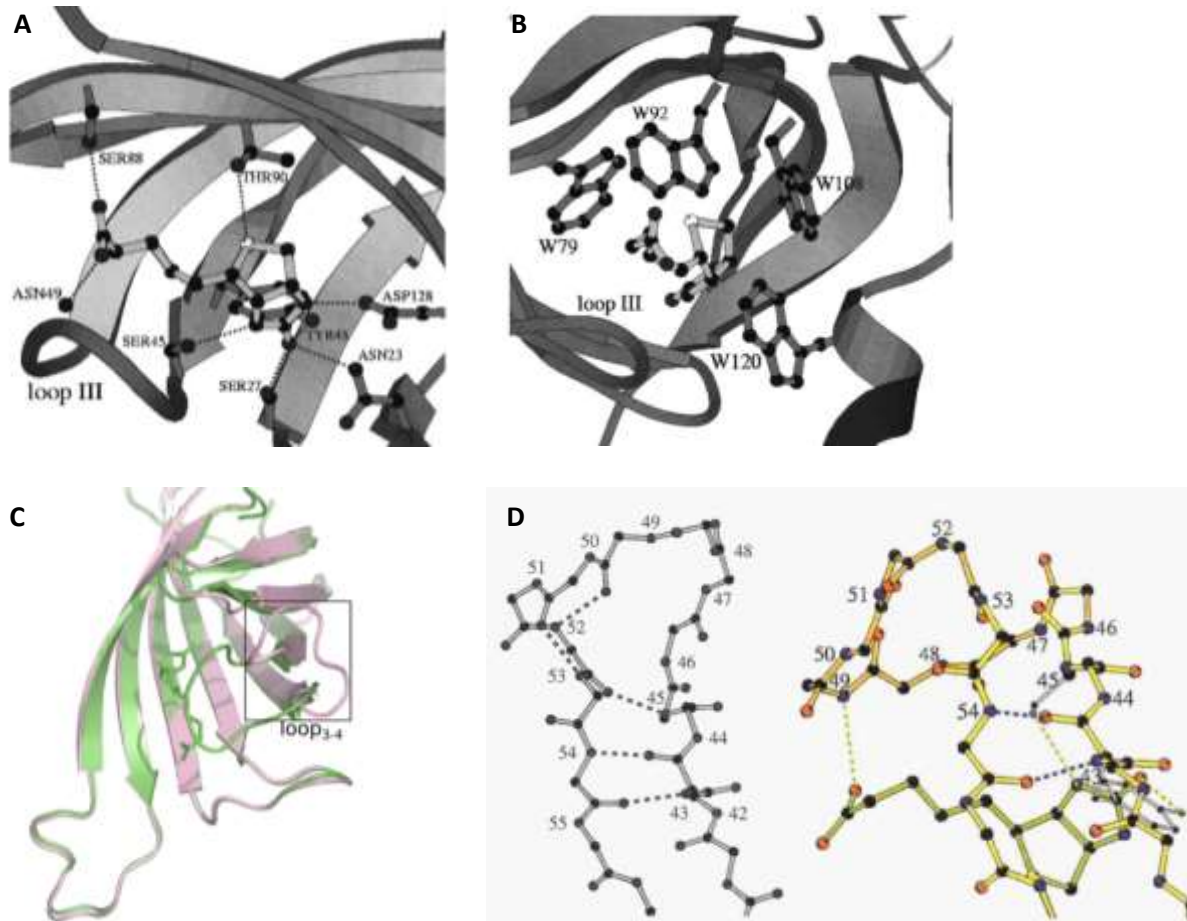


Figure 2: **A.** Hydrogen bonding contacts between SA and biotin in the binding pocket [11]. **B.** Tryptophan contacts between biotin and streptavidin that mediate strong hydrophobic interactions [11]. **C.** Graphical representation of the flexible binding loop₃₋₄ in its open (purple) and closed (green) conformations [10]. **D.** Residue contacts mediating the open (left, black and white) and closed (right, colored) conformations of the binding loop₃₋₄ [12].

Biotin-modification of biological substrates

Biotinylation is the process of covalently linking a biotin molecule to an organic substrate of choice. This is most commonly accomplished through chemical means; although, it can be achieved enzymatically [18]. In general, biotin modifications are most commonly attached to proteins and nucleic acids, but the chemistry of biotinylation allows a biotin tag to be attached to any substrate that can react with the reactive moiety (*Fig. 3A*).

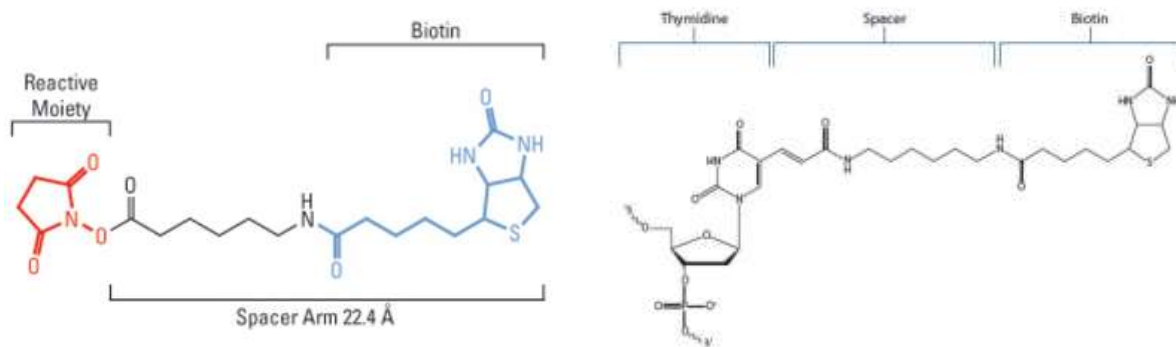


Figure 3: A. Structure of a generic biotinylation reagent containing a non-specific reactive moiety and a relatively short spacer arm [18]. **B.** Structure of Integrated DNA Technologies' internal biotinylated thymidine nucleotide with a 11 Å spacer arm [19]. The Watson-Crick base-pairing face remains intact after biotinylation, and thus this modification can be used for assays involving both single and double stranded DNA.

Both the reactive moiety and spacer arm are variable portions of the biotin modification. For example, more precise reactive moieties can be substituted that only react with specific amino acids or functional groups and the length of the spacer arm can be modified depending on the needs of the project [18]. The length of the spacer arm is particularly important for protein binding of biotinylated compounds, as steric hindrance can have a significant detrimental effect on the strength of streptavidin binding [18].

One of the most useful substrates for biotinylation is DNA. One application for biotinylated DNA bound to SA is to assay the protein displacement ability of certain proteins, such as DNA helicases [20, 21, 22, 23]. Biotin modifications of DNA bases have become readily available from custom oligonucleotide services like Integrated DNA Technologies and ThermoFisher Scientific or they can be added to an oligonucleotide of choice using a biotinylation kit. Such modifications can be placed at the 5' or 3' ends of DNA, or added to internal nucleotides via covalent modification of a thymidine base (biodT) (Fig. 3B) [18]. In the case of biodT, the biotin moiety is attached to the 5' carbon of the thymidine base via a variable length organic spacer arm. When referring to biotinylation, this is the modification that we will be addressing throughout the rest of this paper.

Exploitation of the streptavidin-biotin complex in the laboratory

Not only is the biotin-SA interface incredibly strong, but it is also highly resistant to changes in temperature, pH, and the presence of detergents [14, 24]. For this reason, biotin-SA or biotin-avidin complexes are frequently used in a multitude of biochemical laboratory applications. ELISA (enzyme-linked immunosorbent assays) [25, 26], oligonucleotide labeling [20, 21, 23], immunoprecipitations [1, 27], affinity chromatography [28, 29, 30], DNA sequencing [31], electron microscopy [32, 33], and various types of blotting [34, 35] are just a few of the current applications for the biotin-SA/avidin systems. The potential uses for the exploitation of this complex are nearly endless—and one would be hard-pressed to find a biochemistry laboratory that has not used biotin and SA in one context or another.

Spontaneous dissociation of streptavidin from biotinylated double stranded DNA

Although the biotin-SA interaction is generally believed to be quite robust, we have identified a phenomenon in which the biotinylation of double stranded DNA (dsDNA) results in a very unstable interaction between SA and the biotin modified base. In comparison to biotinylated single stranded DNA (ssDNA), which stably complexes with SA, biotinylated dsDNA dissociates from SA at an anomalously high rate. This phenomenon has also been observed by other groups [20, 21]—however, none of them have attempted to determine why this occurs.

To determine how dsDNA instigates SA dissociation, we first endeavored to determine the rate at which SA dissociates from biotinylated dsDNA relative to its dissociation from biotinylated ssDNA. Using both electrophoretic mobility shift assays (EMSA) and fluorescence polarization assays, we determined the relative dissociation rates for dsDNA compared to ssDNA. Additionally, we explored several differently structured biotinylated DNA constructs to determine if small stretches of ssDNA are sufficient to stabilize SA binding. Eventually, we hope to determine the mechanism by which dsDNA causes the dissociation of SA.

Materials and Methods

The following table outlines each of the DNA sequences that were used at some point in this project along with their corresponding names as referenced in this thesis. Note that assays involving ssDNA (only top strand of a given duplex) will be referred to as “ss[DNA name]” (ex. “ssShort Complement”). Additionally, note that Long Fork, Long Complement, LC1, LC3, and LC5 all contain identical top strands, thus only ssLong Complement will be addressed in later sections.

Name	Sequence
Short Complement	5' -TCCATATCACA/ BiodT /CGAGAATAGATAG -3' 3' -AGGTATAGTGT A GCTCTTATCTATCT-5'
Long Fork	5' -TTGATTAAGTTGGGTAACGCCAGGG/ BiodT /TTTCCCAGTCAA -3' 3' -GATAAGGACGAAGGATAGCACAAATTCAGAAGGCGTACTCACTAATTC AACCC ATTGCGGTCCC A AAAGGGTCAGTTGGG-5'
Short Fork	5' -CCCAACTTAATCACTCATGCGGAC/ BiodT /TAACACGATAGGAAAAAGGAATAC / AlexF488 /-3' 3' -TTTTTTTTTTTTTTTTTTTCGCCTG A ATTGTGCTATCCTTTTCCTTATG -5'
Short Fluor	5' -/ Alex488 /CGCAACT/ BiodT /AATCACTC-3' 3' - GCGTTGA A TTAGTGAG-5'
Long Complement	5' -TTGATTAAGTTGGGTAACGCCAGGG/ BiodT /TTTCCCAGTCAA-3' 3' -AACTAATTC AACCCATTGCGGTCCC A AAAGGGTCAGTT-5'
LC1	5' -TTGATTAAGTTGGGTAACGCCAGGG/ BiodT /TTTCCCAGTCAA-3' 3' -AACTAATTC AACCCATTGCGGTCCC T AAAGGGTCAGTT-5'
LC3	5' -TTGATTAAGTTGGGTAACGCCAGGG/ BiodT /TTTCCCAGTCAA-3' 3' -AACTAATTC AACCCATTGCGGTCCC G T TAAGGGTCAGTT-5'
LC5	5' -TTGATTAAGTTGGGTAACGCCAGGG/ BiodT /TTTCCCAGTCAA-3' 3' -AACTAATTC AACCCATTGCGGTCCC GG T TAAGGGTCAGTT-5'

Table 1: Names and sequences of each DNA construct to be discussed in this thesis. Fluorescent tags are noted in blue and mismatched DNA bases are indicated in red.

1) DNA oligos

Synthetic DNA oligomers were ordered from Integrated DNA Technologies with or without an internal biodT modification (containing a standard length (11 Å) spacer arm). DNA stocks were rehydrated with water and stored at -20 °C until purification.

2) *DNA Purification*

DNA stocks were thawed and mixed with 30% formamide. DNAs were run for 4 to 8 hours (depending on DNA length) at 50 watts on a 15% denaturing (8 M urea) polyacrylamide gel to isolate the primary nucleic acid species. DNA was then visualized using UV light, and DNA bands were cut from the gel. DNA was eluted from the gel in water overnight, and filtered to remove any remaining impurities. Note that unless DNA length exceeded 50 nucleotides, only biotinylated DNA strands were purified, and not their complements. Also note that ssShort Fork DNA was never purified and exhibits significant length variations.

3) *5' radiolabeling of biotinylated DNA and duplex preparation*

Purified DNA was incubated with T4 polynucleotide kinase (PNK) (NEB), T4 PNK buffer (NEB) and [γ -P³²]-ATP (Sigma) at 37 °C for 90 minutes. Then, the enzyme was heat-inactivated at 95 °C for 5 minutes. If duplex DNA was needed, freshly-labeled DNA was incubated with a 1 to 1.1 ratio of its respective complement DNA in 1X annealing buffer (10 mM tris, 6 mM magnesium chloride, and 50 mM sodium chloride). The solution was heated at 95 °C for 5 minutes, then allowed to slow cool to room temperature (23 °C) and stored at -20 °C.

4) *Electrophoretic Mobility Shift Assays (EMSA)*

Labeled single stranded or duplex DNA was incubated in 1X reaction buffer (20 mM HEPES (pH 7.6), 1 mM DTT, 2 mM magnesium chloride, 10 percent glycerol, 20 mM EDTA, 0.01 mg/ml BSA) with or without SA. SA was provided at approximately 8 to 16-fold greater concentration than DNA to ensure that only one DNA molecule would be bound to each SA in solution. Reaction mixtures were incubated at 37 °C for 5 min to facilitate SA binding, then an excess of biotin was added at varying timepoints. All samples were then loaded onto an 8% to 15% non-denaturing polyacrylamide gel and run at 8 watts for 30 to 120 minutes depending on DNA length.

If DNA was radiolabeled, then the gel was exposed and phosphorimaged on a Typhoon gel imager. Otherwise, if the DNA was fluorescently-labeled, the gel was directly imaged on the Typhoon. The resulting gel images were quantitatively analyzed using ImageQuant software.

5) *Fluorescence polarization assays*

a) SA binding assays

Fluorescently-labeled DNA was incubated with 1X reaction buffer and increasing concentrations of SA. The reactions were allowed to equilibrate at 37 °C, then duplicate samples were loaded onto a black-bottomed polystyrene microplate (Corning). The plate was then read by a CLARIOstar microplate reader to obtain fluorescence polarization and anisotropy values for each sample.

b) SA dissociation assays

Fluorescently-labeled DNA was incubated with 1X reaction buffer and SA. SA was supplied at approximately 8 to 16-fold greater concentration than DNA to ensure only one DNA molecule was bound per SA tetramer. The reactions were then allowed to equilibrate at 37 °C for 15 minutes, then duplicate samples were loaded onto a black-bottomed polystyrene microplate (Corning). After plating, an increasing concentration of biotin was added to each well, and the plate was read by a CLARIOstar microplate reader to obtain fluorescence polarization and anisotropy values for each sample.

*All reagents for FP assays were filtered through 2 μ filters before use.

Results

Biotinylated ssDNA binding to SA is stable

In accordance with accepted views regarding the strength and stability of biotin-SA binding, the binding of SA to single stranded biotinylated DNA is exceptionally stable. *Figure 4A* demonstrates that the binding of SA to ssLong Complement is stable up to 50 minutes after adding an excess of free biotin. This stability was also mirrored by other ssDNA complexes such as ssShort Fork (*Fig. 4B*).

Biotinylated duplex DNA dissociates rapidly from SA in the presence of free biotin

Until the addition of free biotin, binding of biotinylated dsDNA to SA is relatively stable, as evidenced by the presence of dsDNA primarily in its bound form in lane 2 of *Figure 6A and B*. However,

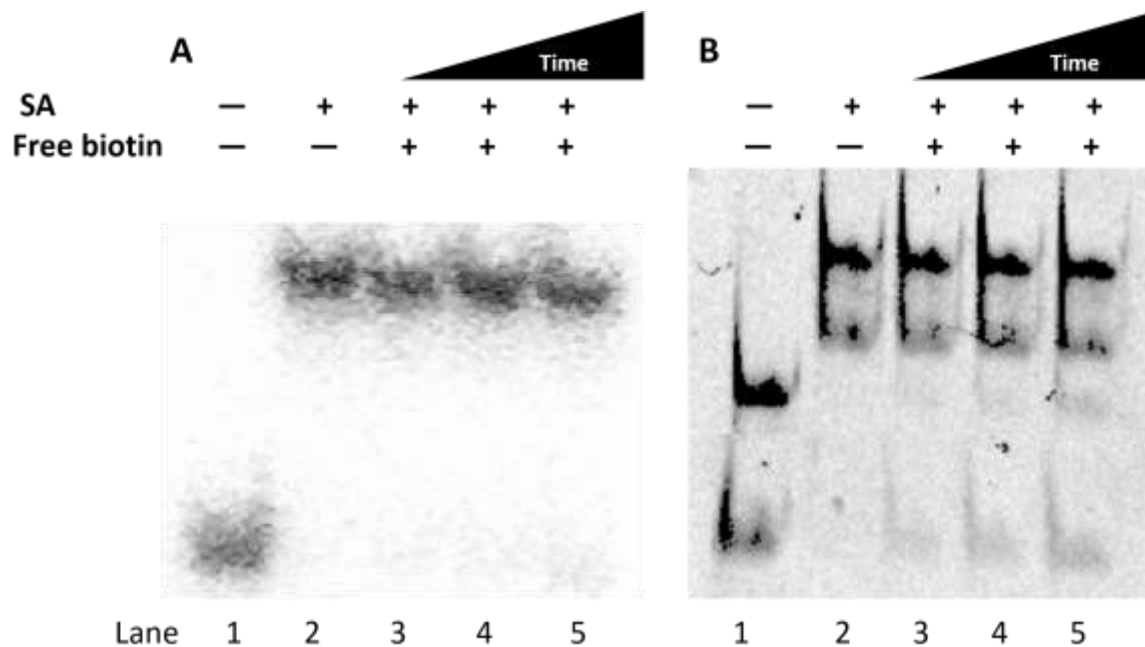


Figure 4 A. EMSA of ssLong Complement stably binding to SA. 160 nM SA was added to 5 nM P³²-labeled DNA in 1X reaction buffer, and 10 μ M free biotin was added at varying timepoints. Samples were all loaded onto the gel at the same time, and lanes 3-5 correspond to 15, 25, and 50 minutes since biotin addition, respectively. *B.* EMSA of ssShort Fork binding to SA. 160 nM SA was added to 5 nM fluorescently-labeled DNA in 1X reaction buffer, and 10 μ M free biotin was added at varying timepoints. Samples were all loaded onto the gel at the same time, and lanes 3-5 correspond to 15, 25, and 50 minutes since biotin addition, respectively. Note that there seems to be significant impurities in ssShort Fork DNA, as it was not purified before use, but both major species appear to bind SA relatively stably.

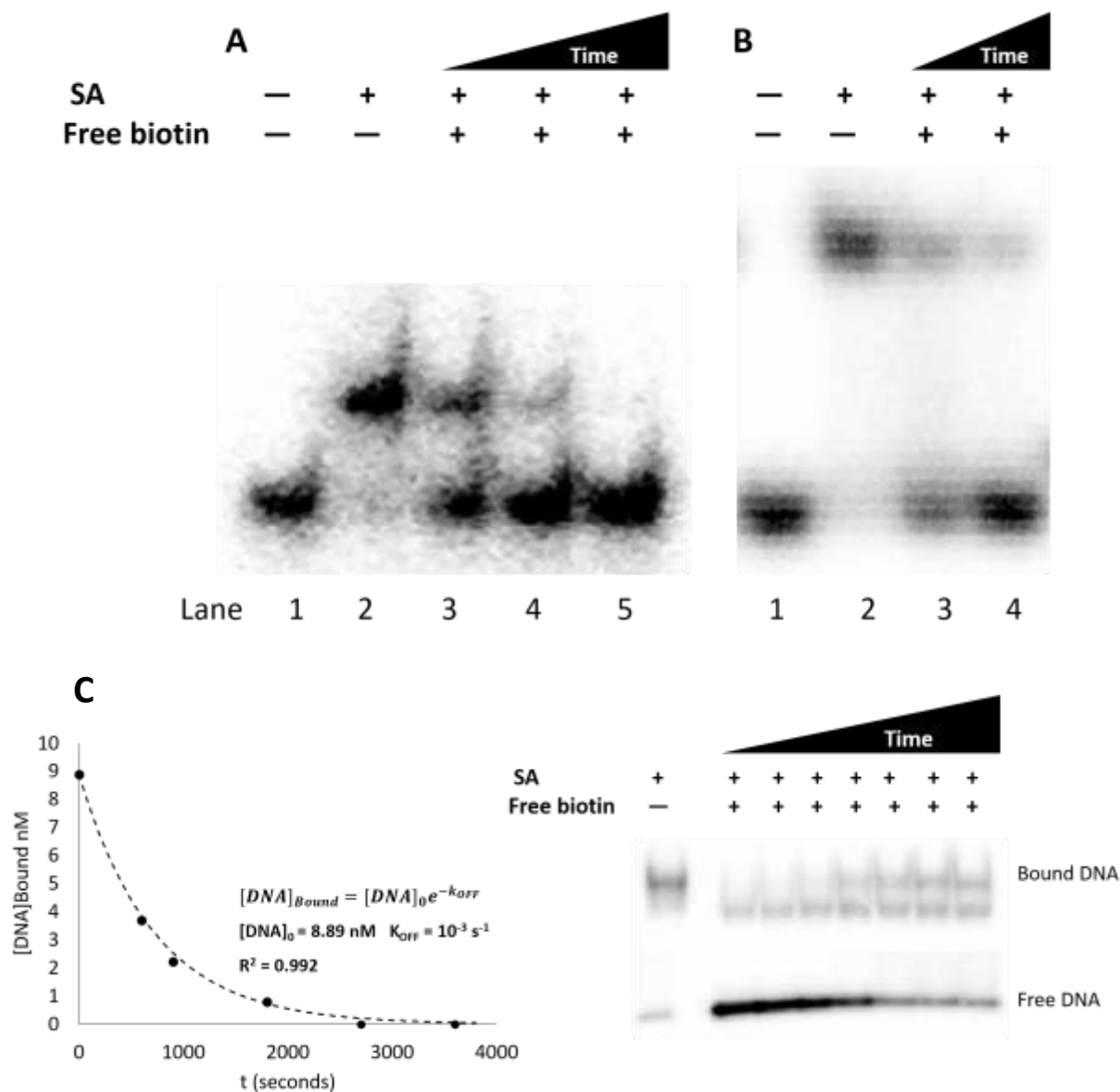


Figure 5 A. Long Fork duplex dissociates from SA rapidly. 160 nM SA was added to 5 nM P³²-labeled DNA in 1X reaction buffer, and 10 μM free biotin was added at varying timepoints. Samples were all loaded onto the gel at the same time, and lanes 3-5 correspond to 15, 25, or 50 minutes since biotin addition, respectively. **B.** Long complement duplex also dissociates from SA rapidly. 160 nM SA was added to 5 nM P³²-labeled DNA in 1X reaction buffer, and 10 μM free biotin was added at varying timepoints. Samples were all loaded onto the gel at the same time, and lanes 3 and 4 correspond to 25 or 50 minutes since biotin addition, respectively. **C.** Determination of k_{OFF} for Short Complement duplex DNA and SA. 160 nM SA was added to 9 nM P³²-labeled DNA in 1X reaction buffer, and 10 μM free biotin was added at varying timepoints. The resulting gel (right) was quantified, then analyzed using Microsoft Excel to fit the data curve (left) and determine k_{OFF} . Note that only the top and bottom bands were used for quantification. The intensity of the middle band appears to remain constant throughout the assay, and thus is believed to be an impurity in the DNA.

upon adding an excess of free biotin, the dsDNA rapidly dissociates and primarily exists in its free form (*Fig. 5A and B* lanes 3-5 and 3-4, respectively). We also attempted to quantify the off-rate of SA from dsDNA, and found that it was approximately 10^{-3} s^{-1} (*Fig. 5C*)—however, this experiment was only conducted once, and thus should be repeated to confirm this off-rate.

Mismatches across from the biotinylation site stabilize SA binding

Given that duplex DNA destabilizes SA binding in the presence of free biotin, we sought out to test whether short stretches of “ssDNA” within a duplex sequence could stabilize binding. As such, we assayed three mismatched DNAs with varying numbers of mismatches (1, 3, or 5 mismatches centered across from the biotinylated site) in addition to their full complement and single stranded counterparts. We found that all three mismatch sequences stabilized SA binding, and even a single mismatch across from biotT was sufficient to achieve this effect (*Fig. 6A and B*).

Short biotinylated oligomers show unusual activity compared to longer DNAs

While investigating SA binding using FP assays, we also noticed that the Short Fluor DNA behaved differently than any of the longer complexes we have investigated—both in terms of its behavior in binding SA as a duplex and as single stranded DNA. Upon the addition of free biotin to the complex of ssShort Fluor, there was significant dissociation of the single-stranded DNA from SA as measured using fluorescence polarization—something that has never been seen for longer ssDNAs (*Fig. 7A and C*). Moreover, full dissociation of the duplex Short Fluor-SA complex upon the addition of free biotin did not occur (*Fig. 7B and C*). These unusual results were also seen for these DNAs with EMSA (*Fig. 7D*).

Additionally, upon determining a binding curve for streptavidin via fluorescence polarization, there was a significant increase in K_D for both ssDNA and dsDNA compared to free biotin. Upon the addition of increasing concentrations of SA, it was found that DNA binding was saturated around a 5:1 ratio of SA to DNA. From this data, we were also able to obtain preliminary K_D values for ssShort Fluor and duplex Short Fluor DNA association with SA of 7 nM and 19 nM, respectively (*Fig. 8A and B*).

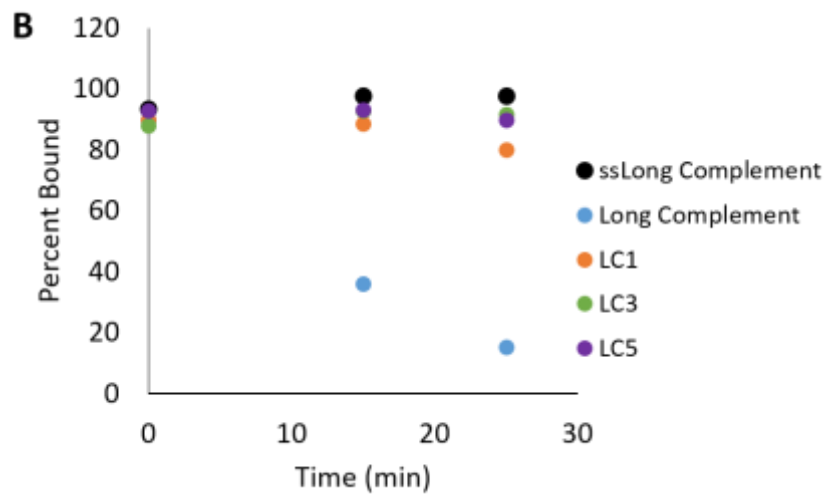
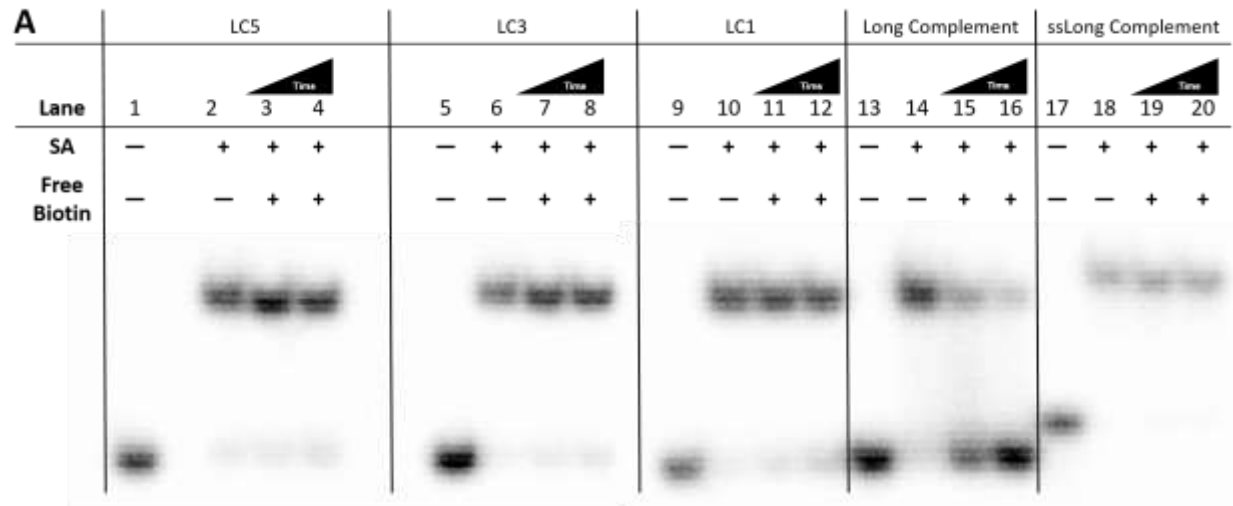


Figure 6 A. EMSA of mismatched DNAs (LC1, LC3, and LC5) as well as their full complement and single stranded counterparts (Long Complement and ssLong Complement). 160 nM SA was added to 5 nM P^{32} -labeled DNA in 1X reaction buffer, and 10 μ M free biotin was added at varying timepoints. Samples were all loaded onto the gel at the same time, and lanes 3, 7, 11, 15, and 19 correspond to 15 minutes since free biotin addition, while lanes 4, 8, 12, 16, and 20 correspond to 25 minutes since free biotin addition. **B.** Quantification of (A) represented in graphical form. Graph was generated in Microsoft Excel.

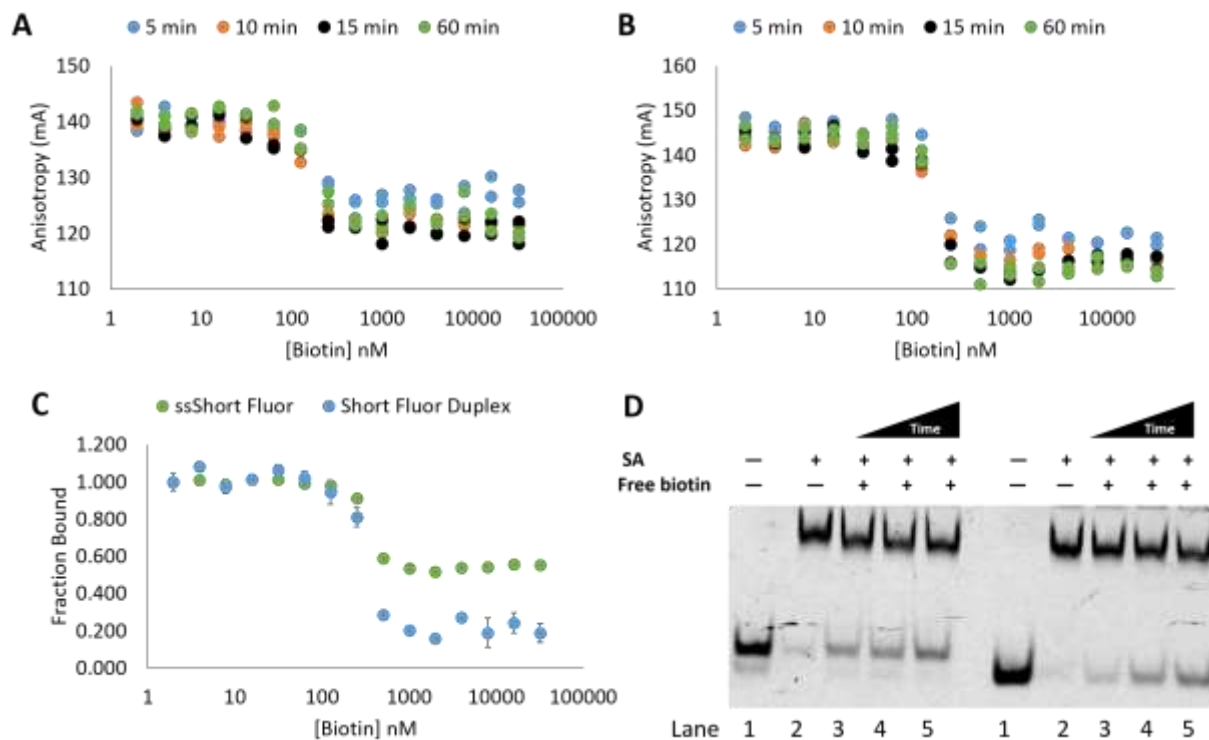


Figure 7 A. Dissociation of ssShort Fluor DNA over time as measured by fluorescence polarization. 160 nM SA was added to 5 nM fluorescently-labeled DNA in 1X reaction buffer, and increasing concentrations of free biotin were added to each individual reaction. Each reaction was run in duplicate and multiple measurements were taken over time. **B.** Dissociation of Short Fluor duplex over time. 160 nM SA was added to 5 nM fluorescently-labeled DNA in 1X reaction buffer, and increasing concentrations of free biotin were added to each individual reaction. Each reaction was run in duplicate and multiple measurements were taken over time. **C.** Fraction bound of both ssShort Fluor and Short Fluor duplex decreases as the concentration of free biotin increases. Duplicate samples from (A) and (B) were averaged, then timepoints 10, 15, and 60 minutes were also averaged. Fraction bound was calculated from changes in anisotropy and plotted versus the concentration of biotin added. Error bars represent the standard deviation of averaged data points. All graphs were generated in Microsoft Excel. **D.** Confirmation of fluorescence polarization results by EMSA of Short Fluor DNA. 160 nM SA was added to 5 nM fluorescently-labeled ssDNA (right lanes 1-5) or dsDNA (left lanes 1-5) in 1X reaction buffer, and 10 μ M free biotin was added at varying timepoints. Lanes 3-5 for both ssDNA and dsDNA correspond to 20, 56, and 96 minutes since free biotin addition, respectively.

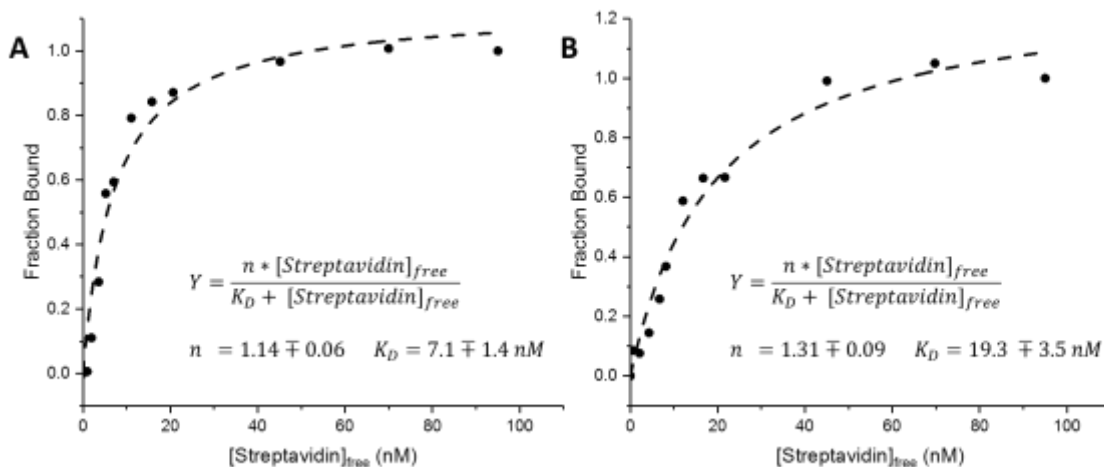


Figure 8 A. ssShort Fluor binding to SA. 5 nM fluorescently-labeled DNA in 1X reaction buffer was added to increasing concentrations of SA. Change in anisotropy was used to calculate the fraction of DNA bound at each concentration and was plotted against the concentration of free SA to determine K_D and n , where n is the number of equivalent binding sites that are occupied. **B.** Short Fluor duplex binding to SA. 5 nM fluorescently-labeled DNA in 1X reaction buffer was added to increasing concentrations of SA. Change in anisotropy was used to calculate the fraction of DNA bound at each concentration and was plotted against the concentration of free SA to determine K_D and n . Graphs were generated and fitted in OriginPro.

Discussion and Conclusions

Given the disparate structures of ssDNA and dsDNA, structural aspects unique to dsDNA are potential candidates for causing the observed dissociation. These include, but are not limited to, the DNA double helix and an increased potential for electrostatic interactions due to the additional phosphate backbone. In particular, the DNA helix gives dsDNA a rigid, rod-like structure, while ssDNA is far more flexible and fluid. As such, steric hindrance due to the rigidity of dsDNA could potentially interfere with SA binding. To partly address this question, we attempted to model the interaction between Long Complement duplex DNA in its β helix form with SA using the molecular modeling program Pymol (Fig. 9). The Long Complement duplex 3D structure was generated online by the make-na server provided by James Stroud [36].

There are many assumptions made in this modeling scheme, including that the biotin modification binds in the same orientation as free biotin and that the DNA helix and SA subunits assume the same conformations under our assay conditions as when they were crystalized. If we consider these assumptions to be correct, however, there are several interesting insights that can be gained from these models.

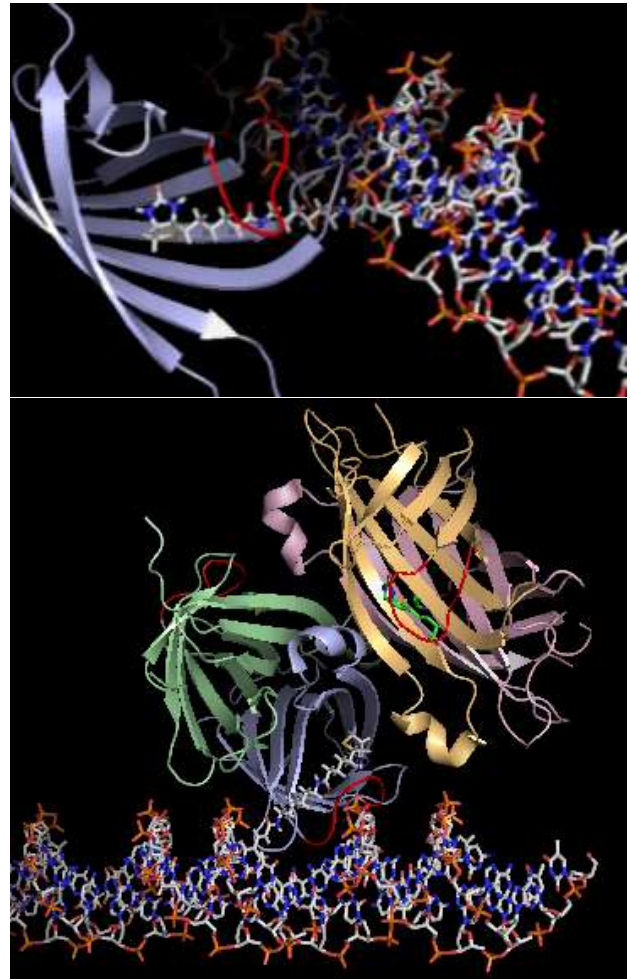


Figure 9 (Top) Theoretical model of one SA subunit's interaction with biodT of Long Complement duplex. (Bottom) Theoretical model of the entire SA tetramer binding to biodT of Long complement duplex DNA, as well as the solved structure of the other subunits binding free biotin. Binding loop₃₋₄ is shown in red for each subunit. Both figures were modified from LeTrong et al. 2011 and renderings were generated in Pymol [7].

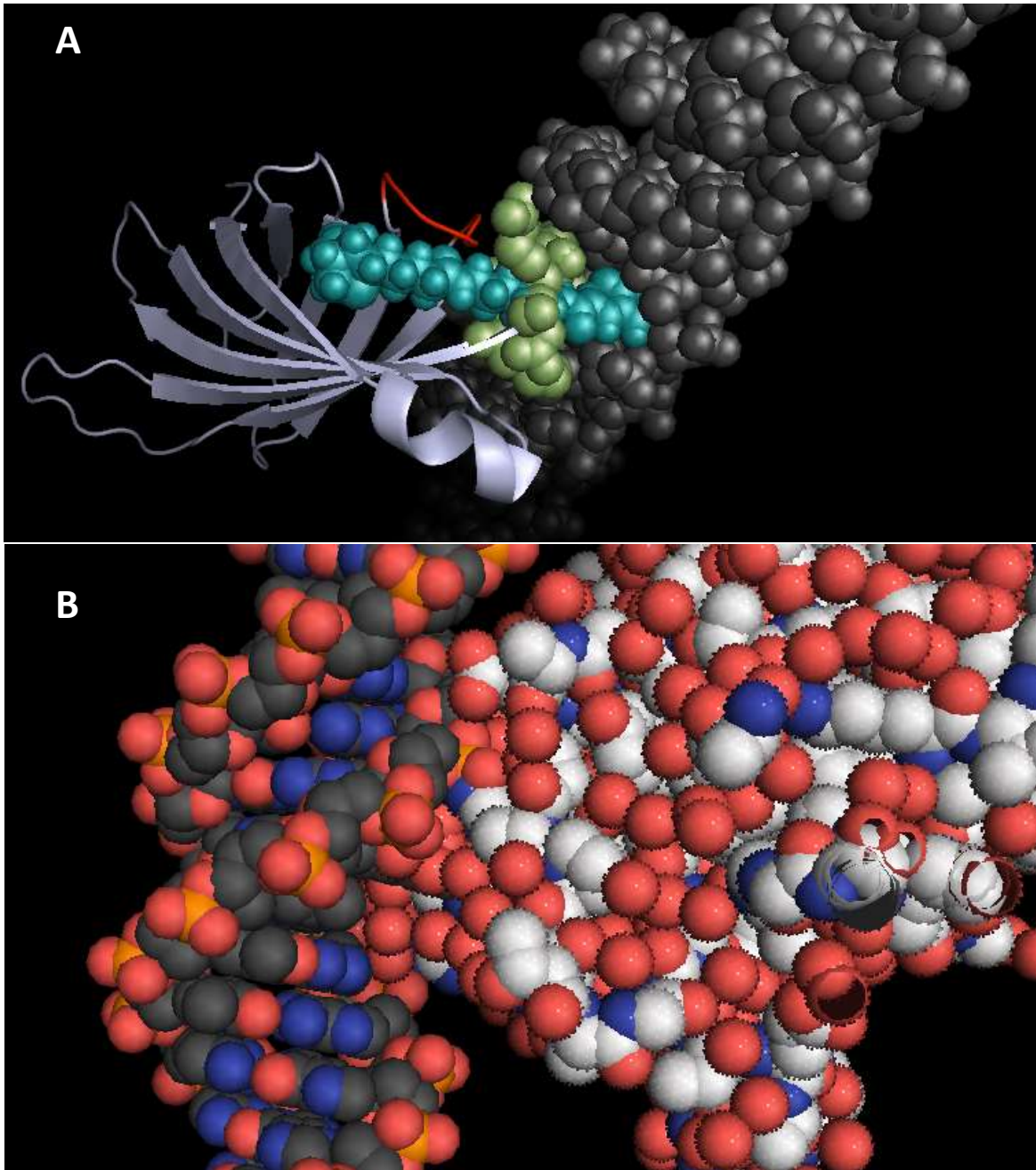


Figure 10 A. Steric hindrance between Long Complement duplex and loop₄₋₅ of the SA subunit. The DNA is represented in space-filling mode in grey with bioT shown in teal, while SA is represented in purple, with only loop₄₋₅ (green) shown in space-filling mode. Binding loop₃₋₄ is shown in red.
B. Potential electrostatic repulsion between the DNA backbone and SA. Both structures are color-coded with red atoms representing oxygen, blue atoms for nitrogen, orange atoms for phosphorus, and grey and white for carbons of DNA and SA, respectively. All figures were modified from Le Trong et al. 2011 and renderings were generated in Pymol [7].

clearance between SA and the biotinylated DNA. Perhaps the other 20 percent of spontaneous dissociation is due to the linker itself—however, why we do not see similar amounts of dissociation for ssDNA remains to be determined.

It should be noted that the fluorescent tag on DNAs used in fluorescence polarization experiments may have interfered with SA binding given that the length of the DNA on either side of the biotin tag is approximately equal to the diameter of SA. Fluorescence polarization assays using Alexa 488-tagged DNA must be relatively short in length to observe changes in anisotropy upon SA binding. Initially, we attempted these assays using the short fork DNA—however, this DNA proved to be too large for such experiments. Given that the Alexa 488 tag has numerous negatively-charged functional groups and has 4 aromatic rings, the fluorescent tag could potentially inhibit binding of ss- and dsDNA to SA given the proximity of the tag to SA due to the short DNA length. Since such dissociation of ssDNA was observed in both fluorescence polarization experiments and EMSA for Short Fluor DNA, but not for Short Fork DNA, it is likely the length of the DNA that is responsible for this phenomenon.

Unfortunately, our modeling is not sophisticated enough to explain why a single mismatch across from the biotinylated site is sufficient to stabilize SA binding. According to Rossetti, transversion mismatches (such as T-T) produce significant local structural alterations of the DNA helix, including

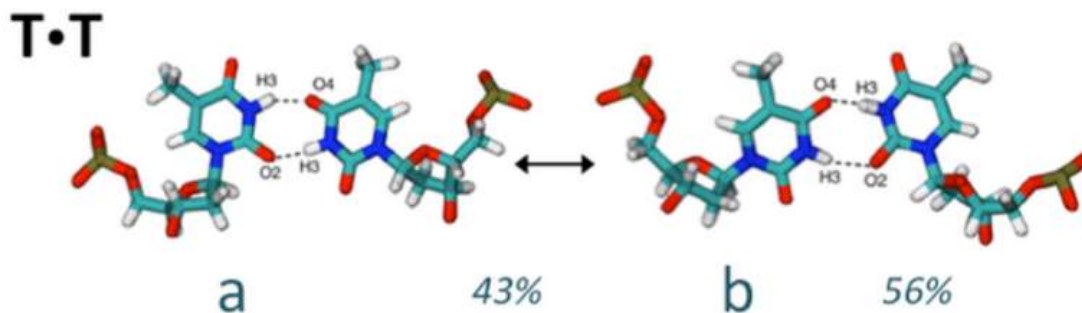


Figure 12 Wobble base pair conformations for T-T mismatches, as well as their relative abundances in solution. Figure reproduced from Rossetti et al. [38].

decreased helical bend, increased breathing, and increased helical twist [38]. Unlike most base mismatches, T-T mismatches form wobble base pairs, rather than bulging out of the DNA helix [38]. This requires local translational movement of the DNA helix, which may be enough to shift the orientation of the biotin spacer arm such that SA binding is no longer sterically impacted. Additionally, T-T mismatches also form two varieties of wobble pairs that are in equilibrium [39] (*Fig. 12*), which makes the DNA more locally fluid. It is possible that these local structural perturbations are sufficient to stabilize SA binding because the mismatch forces the biotin base out of its normal Watson-Crick hydrogen bonding position, thus altering the orientation at which the DNA binds relative to SA. It would certainly be interesting to crystallize the SA-biotinylated dsDNA complex to see if these structural effects do, in fact, impact binding. However, this type of work is beyond the specialties of the Kuchta Lab, as well as the existing time restraints for this project.

Another interesting phenomenon is why SA binding to biotinylated dsDNA is stable until the addition of free biotin. This result could be due to a cooperativity effect of biotin binding to another subunit of the SA. As mentioned previously, the cooperativity of SA binding is a contested topic. It has been found that binding of biotin to SA induces tighter association of the SA subunits via W120, which suggests that the protein exhibits some degree of cooperativity [13, 14]. However, other studies have found that biotin binding is noncooperative [15]. To determine whether cooperativity is involved in SA dissociation, we are currently in the process of procuring a monovalent form of SA from the Ting group at MIT [6]. If, upon the addition of free biotin, SA still rapidly dissociates from dsDNA, then it is likely an effect of the k_{OFF} for the complex—otherwise, cooperativity may be the cause.

In conclusion, the spontaneous dissociation of SA from biotinylated DNA is likely due to a combination of factors. Steric, electrostatic, and potentially cooperative effects may be responsible for this phenomenon, but further investigation is necessary to precisely determine the mechanism by which this occurs. In the meantime, it is useful to know that SA binding to dsDNA can be stabilized by base

mismatches or double biotinylation of the DNA [21]. Thus, SA can still be used to assay for helicase displacement of DNA-bound proteins if the DNA is appropriately modified. However, caution should be taken in other cases where biotinylated dsDNA and SA are being used.

References

1. Avidin-Biotin Interaction. ThermoFisher Scientific, Waltham, Massachusetts, <https://www.thermofisher.com/us/en/home/life-science/protein-biology/protein-biology-learning-center/protein-biology-resource-library/pierce-protein-methods/avidin-biotin-interaction.html> (accessed March 22, 2017).
2. Green, N., Avidin and Streptavidin, *Methods in Enzymology*, **1990**, 184, 51-67.
3. Chivers, C., Crozat, E., Moy, V., Sherratt, D., Howarth M., A streptavidin variant with slower biotin dissociation and increased mechanostability, *Nature Methods*, **2010**, 7(5), 391-393.
4. Wu, S., Wong, S., Engineering Soluble Monomeric Streptavidin with Reversible Binding Capability, *Biological Chemistry*, **2005**, 280(24), 23225-23231.
5. DeMonte, D., Drake, E., Lim, K., Gulick, A., Park, S., Structure-based engineering of streptavidin monomer with a reduced biotin dissociation rate, *Proteins*, **2013**, 1-13.
6. Howarth, M., Chinnapen, D., Gerrow, K., Dorrestein, P., Grandy, M., Kelleher, N., El-Husseini, A., Ting, A., A monovalent streptavidin with a single femtomolar biotin binding site, *Nature Methods*, **2008**, 3(4), 267-273.
7. Le Trong I., Wang Z., Hyre D., Lybrand T., Stayton P., et al., Streptavidin and its biotin complex at atomic resolution. *Acta Crystallographica Section D Biological Crystallography*, **2011**, 67, 813–821.
8. An egg-stremely useful interaction. Protein Data Bank in Europe, Hinxton, Cambridgeshire, UK, <http://www.ebi.ac.uk/pdbe/widgets/QuipStories/avidin/avidin.pdf> (accessed March 22, 2017).
9. Liu, F., Zhang, J., Mei, Y., The origin of the cooperativity in the streptavidin-biotin system: A computational investigation through molecular dynamics solutions, *Scientific Reports*, **2016**, 6.
10. Song, J., Li, Y., Ji, C., Zhang, J., Functional Loop Dynamics of the Streptavidin-Biotin Complex, *Nature Scientific Reports*, **2014**, 5 (7906), 1-10.
11. Stayton P., Freitag S., Klumb L., Chilkoti A., Chu V., et al., Streptavidin-biotin binding energetics, *Biomolecular Engineering*, **1999**, 16, 39–44.
12. Freitag S., Le Trong I., Chilkoti A., Klumb L., Stayton P., et al., Structural studies of binding site tryptophan mutants in the high-affinity streptavidin-biotin complex. *Journal of Molecular Biology*, **1998**, 279, 211–221.
13. Sano T., Cantor, C., Inter subunit contacts made by tryptophan 120 with biotin are essential for both strong biotin binding and biotin-induced tighter subunit association of streptavidin, *Proceedings of the National Academy of Sciences*, **1995**, 92, 3180-3184.

14. Sano, T., Cantor, C., Cooperative Biotin Binding by Streptavidin, *Biological Chemistry*, **1989**, 265(6), 3369-3373.
15. Jones, M., Kurzban, G., Noncooperativity of biotin binding to tetrameric streptavidin, *Biochemistry*, **1995**, 34(37), 11750-11756.
16. Freitag S., Le Trong I., Klumb L., Stayton P., Stenkamp R., Structural studies of the streptavidin binding loop. *Protein Science*, **1997**, 6, 1157–1166.
17. Chu V., Freitag S., Le Trong I., Stenkamp R., Stayton P., Thermodynamic and structural consequences of flexible loop deletion by circular permutation in the streptavidin-biotin system. *Protein Science*, **1998**, 7, 848–859.
18. Biotinylation. ThermoFisher Scientific, Waltham, Massachusetts, <https://www.thermofisher.com/us/en/home/life-science/protein-biology/protein-labeling-crosslinking/protein-labeling/biotinylation.html> (accessed March 22, 2017).
19. Which Biotin Modification to Use? Integrated DNA Technologies, Coralville, Iowa, <http://www.idtdna.com/pages/decoded/decoded-articles/core-concepts/decoded/2012/09/20/which-biotin-modification-to-use->.
20. Yardimici, H., Wang, X., Loveland, A., Tappin, I., Rudner, D., Hurwitz, J., Oijen, A., Walter, J., Bypass of a protein barrier by a replicative DNA helicase, *Nature*, **2012**, 492, 205-211.
21. Bruning, J., Howard, J., McGlynn, P., Use of streptavidin bound to biotinylated DNA structures as model substrates for analysis of nucleoprotein complex distribution by helicases, *Methods*, **2016**, 108, 48-55.
22. Shin, J., Kelman, Z., DNA unwinding assay using streptavidin-bound oligonucleotides, *BMC Molecular Biology*, **2006**, 7(43), 1-8.
23. Morris, P., Raney, K., DNA helicases displace streptavidin from biotin-labeled oligonucleotides, *Biochemistry*, **1999**, 38(16), 5164-5171.
24. Bayer, E., Ben-Hur, H., Gitlin, G., Wilchek, M., An improved method for the single-step purification of streptavidin, *Journal of Biochemical and Biophysical Methods*, **1986**, 13(2), 103-112.
25. Winkler, I., Lochelt, M., Levesque, J., Bodem, J., Flugel, R., Flower, R., A rapid streptavidin-capture ELISA specific for the detection of antibodies to feline foamy virus, *Journal of Immunological Methods*, **1997**, 207(1), 69-77.
26. Bu, D., Zhuang, H., Zhou, X., Yang, G., A heterogeneous biotin-streptavidin-amplified enzyme-linked immunosorbent assay for detecting tris(2,3-dibromopropyl) isocyanurate in natural samples, *Analytical Biochemistry*, **2014**, 462, 51-59.

27. Kim, J., Cantor, A., Orkin, S., Wang, J., Use of in vivo biotinylation to study protein–protein and protein–DNA interactions in mouse embryonic stem cells, *Nature Protocols*, **2009**, 4, 506-517.
28. Rosli, C., Rybak, J., Neri, D., Elia, G., Quantitative recovery of biotinylated proteins from streptavidin-based affinity chromatography resins, *Methods Molecular Biology*, **2008**, 418, 89-100.
29. Herman, T., Lefever, E., Shimkus, M., Affinity chromatography of DNA labeled with chemically cleavable biotinylated nucleotide analogs, *Analytical Biochemistry*, **1986**, 156(1), 48-55.
30. Gretch, D., Suter, M., Stinski, M., The use of biotinylated monoclonal antibodies and streptavidin affinity chromatography to isolate herpesvirus hydrophobic proteins or glycoproteins, *Analytical Biochemistry*, **1987**, 163(1), 270-277.
31. Edwards, J., Itagaki, Y., Ju, J., DNA sequencing using biotinylated dideoxynucleotides and mass spectrometry, *Nucleic Acids Research*, **2001**, 29(21), 1-6.
32. Heitzmann, H., Richards, F., Use of the avidin-biotin complex for specific staining of biological membranes in electron microscopy, *Proceedings of the National Academy of Sciences*, **1974**, 71(9), 3537-3541.
33. Han, B., Walton, R., Song, A., Hwu, P., Stubbs, M., Yannone, S., Arbelaez, P., Dong, M., Glaeser, R., Electron microscopy of biotinylated protein complexes bound to streptavidin monolayer crystals, *Journal of Structural Biology*, **2012**, 180(1), 249-253.
34. Levy-Toledano, R., Caro, L., Hindman, N., Taylor, S., Streptavidin blotting: a sensitive technique to study cell surface proteins; application to investigate autophosphorylation and endocytosis of biotin-labeled insulin receptors, *Endocrinology*, **1993**, 133(4), 1803-1808.
35. Zavala, A., Kulkarni, A., Fortunato, E., A dual color Southern blot to visualize two genomes or genic regions simultaneously, *Journal of Virology Methods*, **2014**, 198, 64-68.
36. Stroud, J., Make-na server. University of New Mexico, Albuquerque, New Mexico, <http://structure.usc.edu/make-na/index.html> (accessed March 15, 2017).
37. Koussa, M., Halvorsen, K., Ward, A., Wong, W., DNA nanoswitches: a quantitative platform for gel-based biomolecular interaction analysis, *Nature Methods*, **2015**, 12 (2), 123-126.
38. Rossetti, G., Dans, P., Gomez-Pinto, I., Ivani, I., Gonzalez, C., Orozco, M., The structural impact of DNA mismatches, *Nucleic Acids Research*, **2015**, 43 (8), 4309-4321.
39. Guoyun, H., Kwok, C., Lam, S., Preferential base pairing modes of T•T mismatches, *FEBS Letters*, **2011**, 585, 3953-3958.